Check for updates

Risk assessment of possible impacts of climate change and irrigation on wheat yield and quality with a modified CERES-Wheat model

Jianchao Liu, Wenbin Yao and Meijun Jiang

ABSTRACT

The effects of climate change on yield and quality in different climate regions have high uncertainty. Risk assessment is an effective measure to assess the seriousness of the projected impacts for decision-makers. A modified quality model was used to simulate integrated impacts of climate change, environment, and management on wheat yield and quality. Then, the Canadian Earth System Model version 5 (CanESM5) was used to forecast the daily meteorological data, and the Statistical Downscaling Model (SDSM V5.2) was used for downscaling. The modified CERES-Wheat was combined with the forecasted meteorological data to simulate the future wheat yield and grain protein concentration (GPC). The risk to wheat yield and quality in three climatic regions in Northwest China under two climate change scenarios of the CanESM5 was assessed. The average temperature increased by 0.22–3.34 °C, and precipitation increased by 10–60 mm from 2018 to 2100. Elevated temperature and precipitation had positive effects on the yields. The risk to yield in most regions with climate change decreased by 3.8–25.1%. The risk to GPC in all regions with climate change decreased by 7.3–27.2%. Irrigation decreased the risk to yield greatly but had different effects in the three climatic regions. The risk to yield with irrigation decreased by 37.7–52.1%. In contrast to previous studies, in this study, the risk to GPC with irrigation substantially increased by 25.8–28.9% in humid regions and 3.9–8.8% in subhumid regions and decreased by 37.7–52.1% in semiarid regions. The irrigation should be discreetly applied for different climatic regions to combat climate change.

Key words | CERES-Wheat, climate change, grain protein concentration, irrigation, wheat yield

Jianchao Liu (corresponding author)
Wenbin Yao
Meijun Jiang
Department of Engineering and Technology, Jiyang College of Zhejiang A and F University, Zhejiang, China
E-mail: *20198001@zafu.edu.cn*

HIGHLIGHTS

- A nitrogen-to-protein conversion factor was added to CERES-Wheat to simulate winter wheat grain protein concentration.
- The combination of general circulation models and CERES-Wheat makes it possible to simulate wheat grain quality with the climate change in landscape levels.
- An irrigation scenario was also used as part of a strategy for responding to climate change in different climatic regions.

This is an Open Access article distributed under the terms of the Creative Commons Attribution Licence (CC BY 4.0), which permits copying, adaptation and redistribution, provided the original work is properly cited (http://creativecommons.org/licenses/by/4.0/).

doi: 10.2166/wcc.2021.248

Downloaded from http://iwaponline.com/jwcc/article-pdf/12/6/2444/935000/jwc0122444.pdf
by guest

INTRODUCTION

In monsoon climates where the annual precipitation fluctuates greatly, the quality and yield of grain are seasonally variable because rainfall is unreliable and there is a significant risk of heat waves during the grain-filling phase (Pleijel *et al.* 2018; Ahmad *et al.* 2020). It is anticipated that under climate change, the growing-season rainfall in many arable cropping regions will change (Dubey *et al.* 2020), and there will be a greater incidence of extreme climatic events (IPCC 2013). The precipitation change in different climatic regions will not be the same because of climate change, but more extreme precipitation events will likely occur (Xu & Liu 2014). At the same time, climate change can result in entirely different effects on grain protein concentration (GPC) (Garofalo *et al.* 2019). GPC is a function of genes, environment, and management. GPC has important effects on nutrition, flour yield, and processing quality (Meng *et al.* 2016). A GPC of approximately 8% is suitable for pastry and cookies, and a GPC of 13–14% is suitable for leavened bread and pasta. Steamed bread and white, salted noodles (Chinese style noodles) should have a medium protein content (approximately 10%) (Addo *et al.* 1991). When the environment or management is less than optimal for wheat, the resulting GPC may not match the intended end use of the wheat (Albert *et al.* 2003).

The artificial climate chamber, open top chamber, and free-air carbon dioxide enrichment methods are the most widely used methods to study the effect of climate change on crop growth (Allen *et al.* 2020). However, these artificial methods are different from the natural environment or are very expensive. The combination of general circulation models (GCMs) and crop models assesses the effects of climate change on cropping systems and is more comprehensive and convenient, but it depends on the progress of the theory (Gilardelli *et al.* 2018). Crop models have often been used to evaluate the effect of climate change on yield (Jabeen *et al.* 2017), but their effect on quality has been rarely reported (Nuttall *et al.* 2017). CERES-Wheat can interpret and simulate nitrogen movement and transfer along the soil–plant–atmosphere continuum, but it cannot output parameters related to quality such as GPC. Many crop models only simulate GPC by a harvest index or the constant nitrogen-to-protein conversion factor (Fp), 5.70 (Zhang *et al.* 2020). It is necessary to add a quality module for crop models to simulate grain quality with different stresses.

GCMs are used for climate prediction (Gaffin *et al.* 2004) but cannot be directly used for climatic studies because of their coarse spatial resolution (Rajabi & Shabanlou 2015). The Canadian Earth System Model version 5 (CanESM5) (Swart *et al.* 2019), based on the Coupled Model Intercomparison Project Phase 5 (CMIP5), and reanalysis from the National Center for Environmental Prediction (NCEP) have been verified in China (Qing *et al.* 2017). The simulation of precipitation and temperature had relatively better results (Song *et al.* 2013). Downscaling is necessary to extract location-scale information from the climatic data downloaded from GCMs (Meenu *et al.* 2013). Statistical downscaling methodologies and dynamical downscaling approaches are common downscaling methods (Schmidli *et al.* 2006). Statistical downscaling methodologies have several advantages, such as low cost, easy operation, and rapid calculation (Timbal *et al.* 2003). The statistical downscaling model (SDSM V5.2) is a statistical downscaling methodology that has been widely used in China (Zhai *et al.* 2016).

Risk is a combination of two factors: the probability that an adverse event will occur and the consequences of the adverse event. Risk assessment encompasses an analysis phase and an implementation phase, risk treatment (Omenn 1997). By comparing the outputs of a multisimulation with a critical threshold, it is possible to evaluate the risk related to future climate conditions. Climate change has important effects on grain quality, but adaptation to climate change has long been neglected in terms of quality. The most commonly used methods to alleviate the impact of climate change are changing the sowing date, using newly cultivated varieties, and implementing reasonable irrigation (Li *et al.* 2011; Worku *et al.* 2018). Irrigation is the most common and simple management approach. Irrigation can improve the nitrogen use efficiency of crops, but it has an adverse effect on winter wheat protein accumulation (Rodríguez-Félix *et al.* 2014).

The wheat yield and quality response to climate change can also vary depending on the location and climate change scenario. Simulation modeling provides an opportunity to understand the broad-scale feedback between climate change

Downloaded from http://iwaponline.com/jwcc/article-pdf/12/6/2444/935000/jwc0122444.pdf
by guest

and agro-production systems at a regional level. In comparison to other models, the modified CERES-Wheat model could better respond GPC to stresses, and the modified CERES-Wheat model was able to simulate GPC with abiotic stress from climate change more precisely. The aims of this study are to assess the risk of climate change to wheat yield and quality and address the risk from irrigation.

MATERIALS AND METHODS

Experimental location and treatments

The field experiment, conducted from October 2014 to June 2017, was located in the Guanzhong irrigation area, and where the average annual precipitation is 580 mm, the average precipitation in the wheat growing season, the average annual temperature, and the annual sunshine duration are 203 mm, 13 °C, and 2,196 h, respectively. The wheat variety 'Xiaoyan 22' (*Triticum aestivum* L.) is widely grown in northwestern and northern China. The four irrigation treatments (I0, rainfed; I1, 60 mm; I2, 120 mm; and I3, 180 mm) involved the whole plots. The four fertilization treatments (N0, 0 kg N ha^{-1}; N1, 105 kg ha^{-1}; N2, 210 kg N ha^{-1}; and N3, 315 kg N ha^{-1}) were the split-plot treatments. Wheat grain samples weighed from 0.1000 to 0.20000 g, and the grain nitrogen content was determined by a Kjeldahl apparatus (JELTEC 2300, Sweden FOSS). The soil samples were collected and dried in an oven to measure the soil water content.

Simulation of GPC based on the modified CERES-Wheat model

The modified CERES-Wheat model is a widely used crop model to simulate wheat development, growth, and yield (Figure 1) (Jones *et al.* 2003). The potential kernel nitrogen accumulation was driven by temperature (Equation (1)) (Ritchie & Otter 1985).

$$\Delta KN_{pot} = \begin{cases} 0.49 \times T_{mean} & T_{mean} \le 10\,^{\circ}C \\ 4.83 + 1.06 \times T_{mean} + 0.25 \times (T_{max} - T_{min}) & T_{mean} > 10\,^{\circ}C \end{cases} \quad (1)$$

where ΔKN_{pot} is the potential kernel nitrogen accumulation, g N $kernel^{-1}$ d^{-1}; T_{max}, T_{min}, and T_{mean} are daily maximum, minimum, and mean temperatures (°C), respectively.

Reference evapotranspiration (ET_0) was calculated by the Priestley–Taylor method (Equations (2) and (3)) (Priestley & Taylor 1972).

$$ET_0 = \alpha E_{EQ} \quad (2)$$

$$E_{EQ} = SR \times 2.04 \times 10^{-4} - ALBEDO \times 1.83 \times 10^{-4} \times (T_{MAX} \times 0.6 + T_{MIN} \times 0.4 + 29.0) \quad (3)$$

where α is a coefficient of advection, dimensionless; SR is the daily total solar radiation, MJ m^{-2} d^{-1}; ALBEDO is the crop albedo, dimensionless; E_{EQ} is equilibrium evapotranspiration, MJ m^{-2} d^{-1}.

The modified CERES-Wheat could simulate the wheat grain yield at maturity (YIELD), grain nitrogen yield at maturity (GNAM), water stress (S_W), and nitrogen stress (S_N). The calculation of Fp (Equation (4)) was determined by S_W and S_N in the previous study, which increased the precision of the simulation of GPC (Liu *et al.* 2018). The dynamic Fp reflected the influence of water and nitrogen stress more accurately, and the accuracy of GPC improved 26.5%. GPC (Equation (5)) was simulated by the GNAM, yield, and Fp, as follows (McKenzie *et al.* 2006):

$$Fp = -5.46 \times MIN(S_W, S_N) + 5.72 \quad (4)$$

$$GPC = \frac{GNAM}{YIELD} \times Fp \times 100 \quad (5)$$

where Fp is the nitrogen-to-protein conversion factor, dimensionless; S_W is the water stress factor, dimensionless; and S_N is the nitrogen stress factor, dimensionless.

Weather data

Daily maximum and minimum temperature (°C), precipitation (mm), and solar radiation (MJ m^{-2} d^{-1}) are the essential weather data for CERES-Wheat (Jones *et al.* 2003). The weather data included historical weather data and climate scenario data.

Historical weather data

Historical weather data (1957–2017) were obtained from the China Meteorological Data Network (http://data.cma.cn/site/index.html), including daily maximum and minimum temperature, precipitation, and sunshine hours. The daily solar radiation data required by the crop model were calculated at the site level using the Angstrom–Prescott equation (Wong & Chow 2001).

Downloaded from http://iwaponline.com/jwcc/article-pdf/12/6/2444/935000/jwc0122444.pdf
by guest

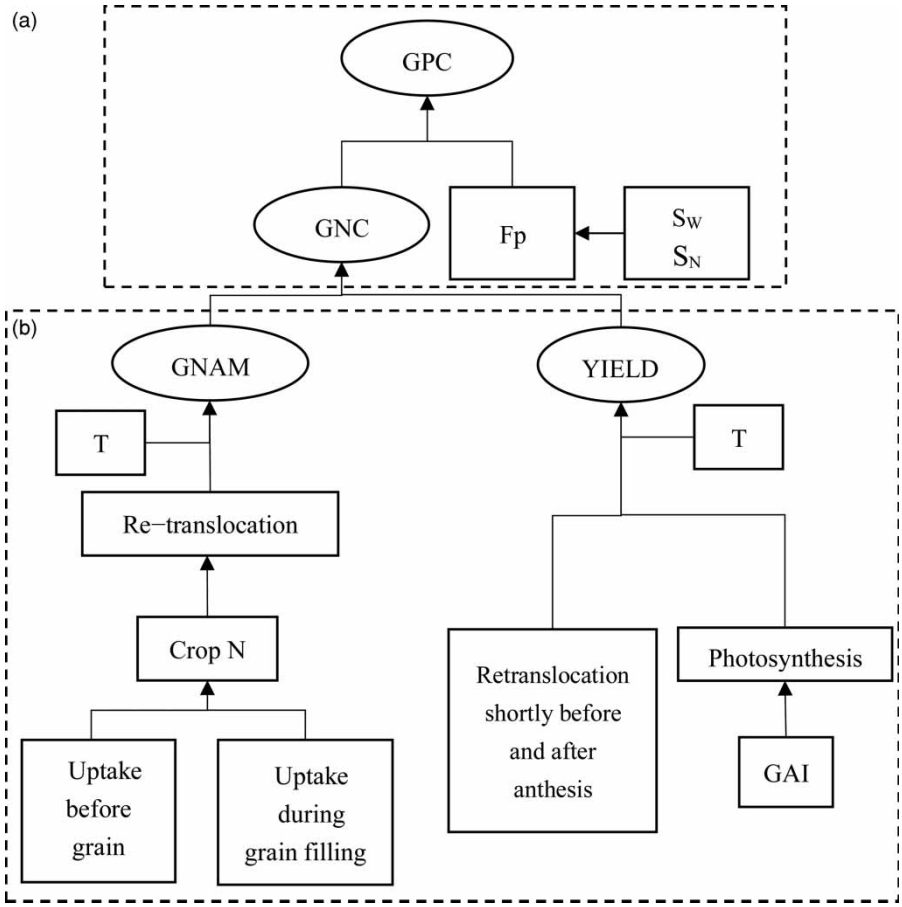

Figure 1 | CERES-Wheat structure (a) for grain nitrogen yield at maturity (NUCM) and grain yield at maturity (HWAM) simulation and GPC (b) for GNC and GPC. (Fp, nitrogen-to-protein conversion factor; *T*, temperature; GAI, green leaf area index; S_W, water stress; S_N, nitrogen stress).

Climate scenario data

The future climate scenario data were produced from global climate models (GCMs) from the Coupled Model Intercomparison Project phase 6 (CMIP6) (Eyring *et al.* 2016). These future climate scenario data will be driven by CMIP6 models under combined SSPs and RCPs (O'Neill *et al.* 2014). In this study, we considered two integrated scenarios (combining SSP2 with RCP4.5 which is defined by SSP2-4.5, and combining SSP5 with RCP8.5 which is defined by SSP5-8.5). The two intermediate scenarios were more suitable for China because of its economic development, greenhouse gas emissions, and land use (Xin 2017). SSP2 presupposes a central pathway in which trends continue their historical patterns without substantial deviations. SSP5 presupposes relatively optimistic trends for human development, with substantial investments in education and health, rapid economic growth, and well-functioning institutions (Bai *et al.* 2021). RCP4.5 is radiative forcing 4.5 Watts m^{-2}, and RCP8.5 is radiative forcing 8.5 Watts m^{-2}. The climate change scenario was obtained using CanESM5 at a grid size of 2.8125°. The reanalysis weather data of the climatic scenario were downloaded from the NCEP. These data included 26 atmospheric predictor variables (e.g., mean sea level pressure, 850 hPa zonal velocity, total precipitation, and mean temperature at 2 m) for 1961–2017 and GCM projections for the SSP2-4.5 and 5-8.5 from 2018 to 2100.

Calibration and validation

Calibration was completed running GLUE (He *et al.* 2009). Related data were from a treatment of sufficient irrigation and sufficient fertilization (I3N3) in 2014.

Model validation was completed by comparing measured and simulated soil water content, yield, and GPC for 2015–

Downloaded from http://iwaponline.com/jwcc/article-pdf/12/6/2444/935000/jwc0122444.pdf
by guest

2017. Three evaluation indicators were used to test the accuracy. The percent deviation (d) was smaller, and the simulated values were better. The smaller the relative root mean square error (RRMSE) (Equation (6)) was, the smaller the difference in the measured and simulated values (0–10%, excellent; 10–20%, good; 20–30%, fair and >30%, poor). In addition, r^2 was used to assess the downscaled climatic projection, and the best index was 1.

$$\mathrm{RRMSE} = \frac{\sqrt{\sum_{i=1}^{n} \frac{(s_i - o_i)^2}{n}}}{\sum_{i=1}^{n} \frac{o_i}{n}} \times 100\% \quad (6)$$

where s_i is the simulated value, o_i is the observed value, and n is the sample size.

Scenarios

Due to the long and narrow topography in Shaanxi Province, different cropping systems are used in different regions. To ensure the results were explanatory and uniform, the management parameters were set as follows: fertilization was 210 kg N ha^{-1} before sowing; the sowing dates were 1–15 October when the daily average temperature was above 20 °C and precipitation was less than 2 mm; the cultivation method was rotary tillage; the plant population density was 240 seeds m^{-2}; and the harvesting time occurred when winter wheat had matured. The scenarios included irrigation (60 mm during wheat wintering and 60 mm during the elongation stage) and rainfed (no irrigation). Soil data from 12 locations were used for modified CERES-Wheat and collected from the China Soil Database (http://vdb3.soil.csdb.cn/) (Table 1). The change in CO_2 concentration was not considered. A greater uncertainty in simulating wheat yields under climate change was due to the response mechanism of rising CO_2 concentrations than to the variations among the downscaled GCMs (Asseng *et al.* 2013).

Risk assessment

To estimate the risk to wheat yield and quality, the yield and GPC were compared with a critical threshold, which is calculated as the 60-year mean yield and GPC for the historical period (1957–2017). The risk to wheat yield and GPC shortfall was then defined as the relative frequency of yield and GPC below the threshold, representing the likelihood of future yield and GPC being lower than the historical mean yield and GPC. The risk to yield (Equation (7)) and GPC (Equation (8)) were estimated as:

$$M_i = \begin{cases} 1, & Y_i \le \overline{Y} \\ 0, & Y_i > \overline{Y} \end{cases} \quad \text{and} \quad R = \frac{\sum_{i=1}^{n} M_i}{n} \times 100\% \quad (7)$$

$$M'_i = \begin{cases} 1, & \mathrm{GPC}_i \le \overline{\mathrm{GPC}} \\ 0, & \mathrm{GPC}_i > \overline{\mathrm{GPC}} \end{cases} \quad \text{and} \quad R' = \frac{\sum_{i=1}^{n} M'_i}{n} \times 100\% \quad (8)$$

where R and R' are the risk to yield and GPC, respectively, %; M and M' are the determination factors of yield and

Table 1 | Twelve site locations in Shaanxi, China, and their climatic information

Climate	Site	Latitude (°)	Longitude (°)	Altitude (m)	Soil organic matter (%)	Mean temperature during growing period (°C)	Precipitation during growing period (mm)
Humid	Ankang (AK)	32.7	109	895	1.56	11.6	316.0
	Hanzhong (HZ)	33.1	107.1	895	1.56	10.3	352.5
	Fopimh (FP)	33.6	108	1,840	1.75	8.8	310.2
	Shangluo (SL)	33.9	110	1,100	1.31	8.9	273.8
Semi-humid	Wugong (WG)	34.3	108.2	426	1.14	8.7	228.1
	Fengxiang (FX)	34.5	107.4	690	1.23	8.0	184.9
	Tongchuan (TC)	35.1	109.1	1,040	1.36	6.3	206.7
	Yanan (YA)	36.6	109.5	1,146	0.92	5.5	152.0
Semiarid	Wuqi (WQ)	36.9	108.2	1,060	0.87	3.2	150.8
	Suide (SD)	37.5	110.2	1,052	0.48	4.6	121.8
	Dingbian (DB)	37.6	107.6	1,500	0.54	3.9	95.7
	Yulin (YL)	38.3	109.8	1,400	0.84	2.9	102.9

Downloaded from http://iwaponline.com/jwcc/article-pdf/12/6/2444/935000/jwc0122444.pdf
by guest

GPC, respectively; Y is yield, kg ha^{-1}; is the $\overline{Y}$ 60-year mean yield for the historical period (1957–2017), kg ha^{-1}; GPC is the grain protein content, %; $\overline{GPC}$ is the 60-year mean GPC for the historical period (1957–2017), %.

RESULTS

Calibration and validation

Modified CERES-Wheat

The percent deviation values between the simulated and observed phenological period, yield, grain nitrogen concentration, and evapotranspiration (ET) were all less than 10%, implying that the model simulated the phenology, wheat growth, nitrogen transformation, and water transformation well (Table 2). The genetic coefficients were relatively stable and could be used in the same or similar 12 sites.

Comparing the simulated values with the observed values of ET (Figure 2(a)), yield (Figure 2(b)), and GPC (Figure 2(c)) in the 16 treatments from 2015 to 2016, the data were distributed near the 1:1 line; the RRMSE values were 9.6, 3.5 and 7.0%, respectively. The values were all less than 10%, so modified CERES-Wheat simulated water and nitrogen stress against winter wheat ET, yield, and GPC well. However, modified CERES-Wheat underestimated the effects of severe nitrogen stress (N0), as the observed values were greater than the simulated values. GPC was overestimated with slight nitrogen stress (N1).

Statistical downscaling model

The daily maximum temperature, daily minimum temperature, monthly total precipitation, and monthly total radiation downscaling were selected as the predictor variables. The SDSM was calibrated from 1961 to 1990 using these predictors. To validate the reliability of the calibrated SDSM, the simulated result from 1991 to 2017 was compared with the observed data from 1991 to 2017. The coefficient of determination (r^2) for these linear relationships varied from 0.64 to 0.93 (Table 3). A very significant power correlation between the predictand and predictor variables ($p < 0.001$ level) was evident.

Analysis of historical and future climate

The terrain of Shannxi is long and narrow, and the latitude range is very large. The annual average temperature (1957–2017) is 2.8–11.6 °C during the wheat growing season. The temperature to the south is higher and gradually decreases from south to north (Figure 3(a)). The subhumid and semiarid regions warmed relatively faster and increased by 0.92 °C in SSP2-4.5. Tongchuan in the subhumid region experienced a 1.01 °C increase. The smallest increase for a location occurred in Fengxiang in the subhumid region, which increased by 0.22 °C. The speed of increase was consistent throughout Shaanxi in SSP5-8.5 where the temperature increased by 0.85–0.98 °C compared with that under SSP2-4.5. The temperatures of Yanan, Wuqi, and Tongchuan in the subhumid region increased the most rapidly by 1.80, 2.05, and 3.34 °C, respectively. The situations in the humid and semiarid regions were the same, as the average temperature increased by 1.70 °C.

The precipitation during the growth period gradually decreased from south to north. The available precipitation in the semiarid region during the growth period was scarcer than that in the other regions (Figure 3(b)). Precipitation in all regions increased under SSP2-4.5. However, for some locations, such as Wuqi, precipitation decreased very little. The precipitation situation was similar to SSP5-8.5. The average precipitation during the growth period increased

Table 2 | Calibration results of the treatment with sufficient irrigation and fertilization in 2014

Anthesis (DAS)			Maturity (DAS)			Yield (kg hm^{-2})			GNC (kg N hm^{-2})			ET (mm)		
Sim.	Obs.	*d* (%)	Sim.	Obs.	*d* (%)	Sim.	Obs.	*d* (%)	Sim.	Obs.	*d* (%)	Sim.	Obs.	*d* (%)
199	199	0	233	233	0	8,025	8,287	− 3.16	165	169	− 5.22	458	469	− 2.34

Note: Sim., simulated values; Obs., observed values; *d*, percent deviation values; DAS, days after sowing; GNC, grain nitrogen concentration; ET, evapotranspiration.

Downloaded from http://iwaponline.com/jwcc/article-pdf/12/6/2444/935000/jwc0122444.pdf
by guest

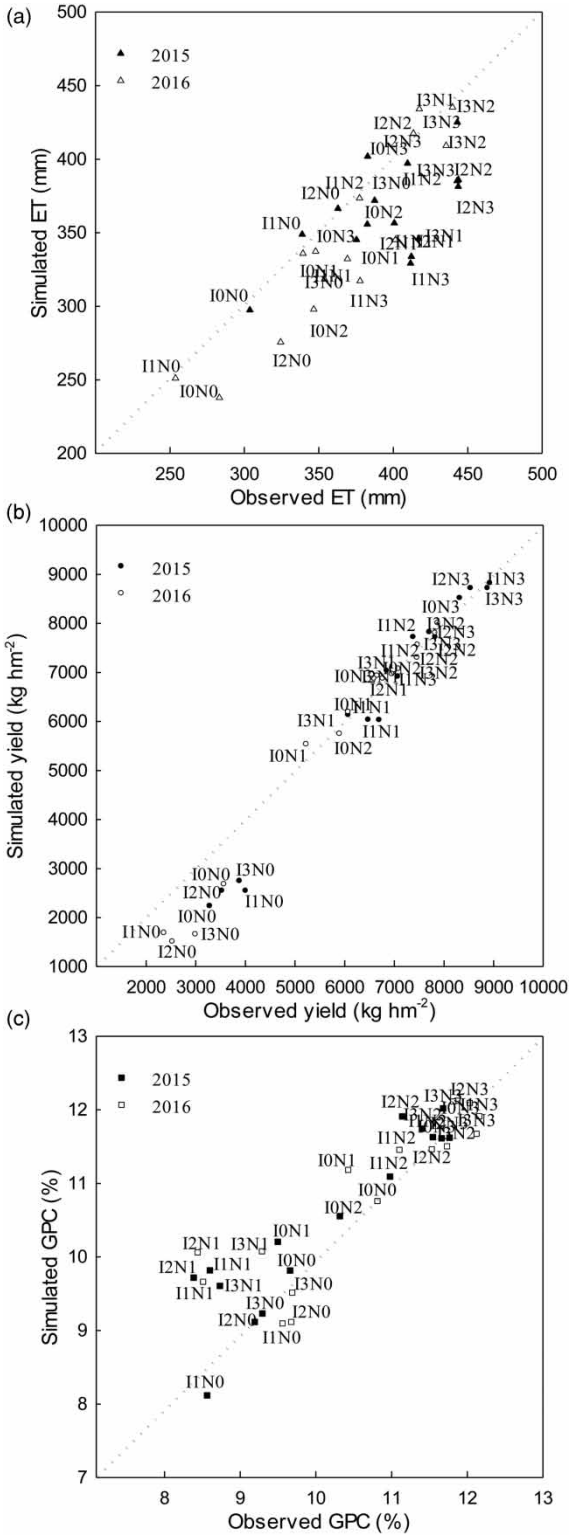

Figure 2 | Observed values vs. simulated values of ET (a) from 2015 (▲) to 2016 (△), yield (b) from 2015 (●) to 2016 (○), and GPC (c) from 2015 (■) to 2016 (□) for 16 different irrigation and fertilization treatments during the two growing seasons of 2015 and 2016. The dotted line is the 1:1 line.

by approximately 13% compared with the amount of historical precipitation.

Phenology

Phenology was derived by accumulated temperature in CERES-Wheat; therefore, higher temperatures always mean a quicker growth. The flowering stage and the mature stage under SSP2-4.5 and SSP5-8.5 occurred relatively earlier (Figure 4(a) and 4(b)). The performances of the three climatic regions were similar. The grain-filling duration in the humid region was almost constant with climate change (Figure 4(c)). However, the grain-filling duration in the subhumid and semiarid regions under SSP2-4.5 and SSP5-8.5 occurred earlier.

Winter wheat yield and risk

Winter wheat yield with latitude increasingly showed a tendency of increasing first and then decreasing. The average historical yield at the 12 locations ranged from 3,849 to 9,434 kg ha^{-1} and had extreme variation under rainfed conditions. The maximum yields were 9,434 and 9,025 kg ha^{-1} in Fuping and Shangluo in the humid region, respectively. The minimum yield was 3,849 kg ha^{-1} in Wuqi in the semiarid region (Figure 5).

The average yield in the humid region decreased by 0.2–14.1% under SSP2-4.5. In comparison to that in the eastern area, the average yield in the western area of the humid region significantly declined more. The yield in the southern part of the subhumid region also decreased by 0.4–1.0%, but the yield in the northern part increased by 16.1–52.7%. The yield in the semiarid region increased slightly by 7.5–10.3%. The average yield under SSP5-8.5 in the humid region and the southern subhumid region increased slightly, but both yields were lower than the historical yield; the yields of the northern subhumid region and the semiarid region increased significantly.

Irrigation significantly changed the impact of climate change on yield. However, with the coupling effects of irrigation and climate change, the yield in the humid region decreased with increasing radiative forcing, but the yield in the semiarid region increased. The yield of the subhumid region remained approximately the same.

Downloaded from http://iwaponline.com/jwcc/article-pdf/12/6/2444/935000/jwc0122444.pdf
by guest

Table 3 | Number and r^2 of calibration periods and validation periods for temperature, precipitation, and radiation between predicted variables and predictor variables

Predicted variables	Predictor variables (NCEP reanalysis)	Calibration periods		Validation periods	
		Number	r^2	Number	r^2
T_{max}	Mean sea level pressure, specific humidity at 850 hPa, wind strength at 850 hPa, southerly wind at 850 hPa, the surface zonal velocity component, 850 hPa height zonal velocity component	10,957	0.8718	5,479	0.8088
T_{min}	Mean sea level pressure, the surface zonal velocity component, 500 hPa height geostrophic air-flow velocity, 500 hPa geopotential height, 850 hPa height zonal velocity component, near-surface specific humidity	10,957	0.9429	5,479	0.9301
Precipitation	The surface meridional velocity component, 500 hPa height meridional velocity component, specific humidity at 500 hPa height, near-surface specific humidity	360	0.6373	180	0.5465
Radiation	Mean sea level pressure, 500 hPa height meridional velocity component, 500 hPa geopotential height, 500 hPa height wind direction, 850 hPa geopotential height, mean temperature at 2 m	360	0.8857	180	0.9018

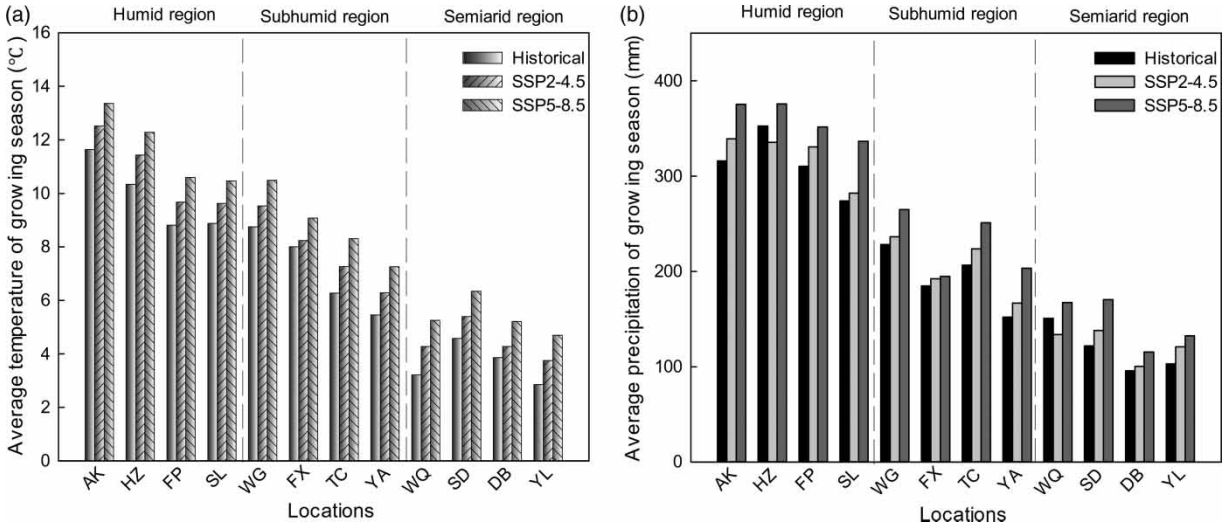

Figure 3 | Average temperature (a) and precipitation (b) under the historical climate over 60 years (1957–2017) (first column), radiative forcing at 4.5 Watts m^{-2} for 82 years (2018–2100) (SSP2-4.5) (second column), and radiative forcing at 8.5 Watts m^{-2} for 82 years (2018–2100) (SSP5-8.5) (third column).

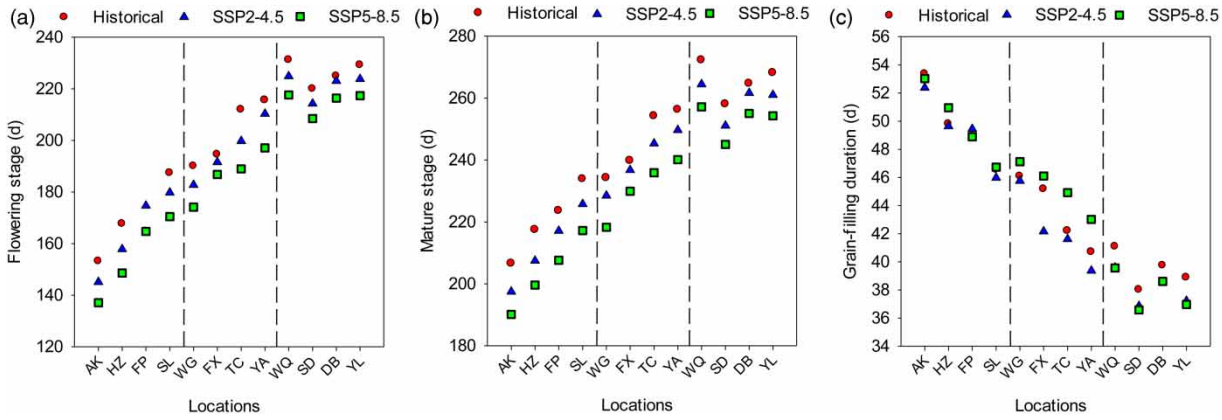

Figure 4 | Flowering stage (a), mature stage (b), and grain-filling duration (c) under the historical climate over 60 years (1957–2017) (●), radiative forcing at 4.5 Watts m^{-2} for 82 years (2018–2100) (SSP2-4.5) (▲), and radiative forcing at 8.5 Watts m^{-2} for 82 years (2018–2100) (SSP5-8.5) (■).

Downloaded from http://iwaponline.com/jwcc/article-pdf/12/6/2444/935000/jwc0122444.pdf
by guest

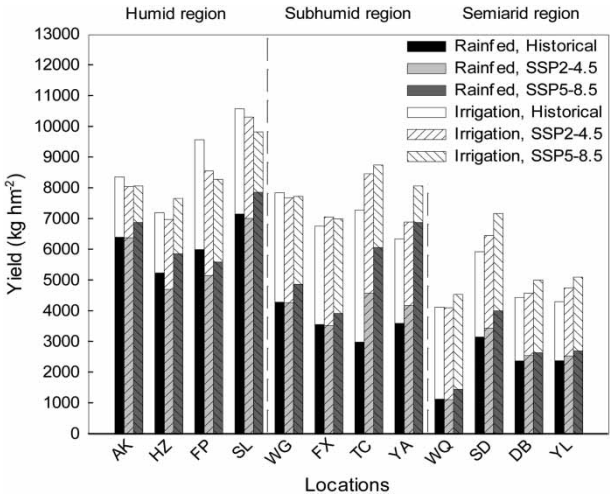

Figure 5 | Rain fed (different gray levels) and irrigated (different gradients) winter wheat yield under the historical climate over 60 years (1957–2017) (first column), radiative forcing at 4.5 Watts m^{-2} for 82 years (2018–2100) (SSP2-4.5) (second column), and radiative forcing at 8.5 Watts m^{-2} for 82 years (2018–2100) (SSP5-8.5) (third column).

The risk to yield in the humid region increased 3.8% under SSP2-4.5 (Figure 6(a)). The risk to yield in the subhumid region and semiarid region under SSP2-4.5 decreased by 12.8 and 5.9%, respectively. The risk to yield in the humid region, subhumid region, and semiarid region under SSP5-8.5 decreased by 12.8, 15.7, and 25.1%, respectively. The yield risk with irrigation decreased by 52.1% under the historical climate, by 50.5% under SSP2-4.5, and by 37.7% under SSP5-8.5 (Figure 6(b)).

Grain protein content and risk

The historical GPC decreased from south to north first and then increased (Figure 7(a)). That of the humid and semiarid regions increased to 11.69 and 11.88% under SSP2-4.5, respectively. However, the GPC in the subhumid region decreased to 10.94% (Figure 7(b)). With the continuously increasing radiative forcing, the GPC of the humid and semiarid regions unexpectedly decreased to 11.49 and 11.27% under SSP5-8.5, respectively (Figure 7(c)). The GPC in the subhumid region increased to 10.97%.

Irrigation had a negative effect on the GPC in the humid and subhumid regions and a positive effect on GPC in the semiarid region (Figure 8). The GPC of the humid and subhumid regions decreased by 1.11 and 0.81%, respectively. However, the GPC of the semiarid region increased 0.77% (Figure 8(a)). The historical GPCs of Fuping, Shangluo, and Xi'an in central Shaanxi were the lowest.

With the coupling effect of irrigation and climate change, the GPC of the three regions had a different response. The average historical GPC of the semiarid region was 11.76%. However, the average historical GPC of the humid and subhumid regions was only 10.09 and 10.45%, respectively. The GPC of the humid and subhumid regions was only slightly different. However, the GPC of the humid region increased 10.09–10.60% with the increase in radiative forcing, whereas the GPC of the subhumid region

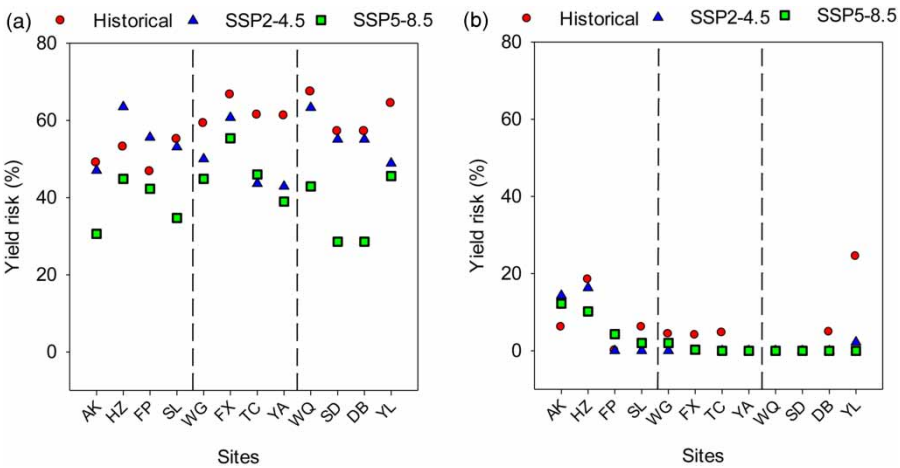

Figure 6 | Risk to yield from rainfed conditions (a) and irrigation (b) under the historical climate over 60 years (1957–2017) (●), radiative forcing at 4.5 Watts m^{-2} for 82 years (2018–2100) (SSP2-4.5) (▲), and radiative forcing at 8.5 Watts m^{-2} for 82 years (2018–2100) (SSP5-8.5) (■).

Downloaded from http://iwaponline.com/jwcc/article-pdf/12/6/2444/935000/jwc0122444.pdf
by guest

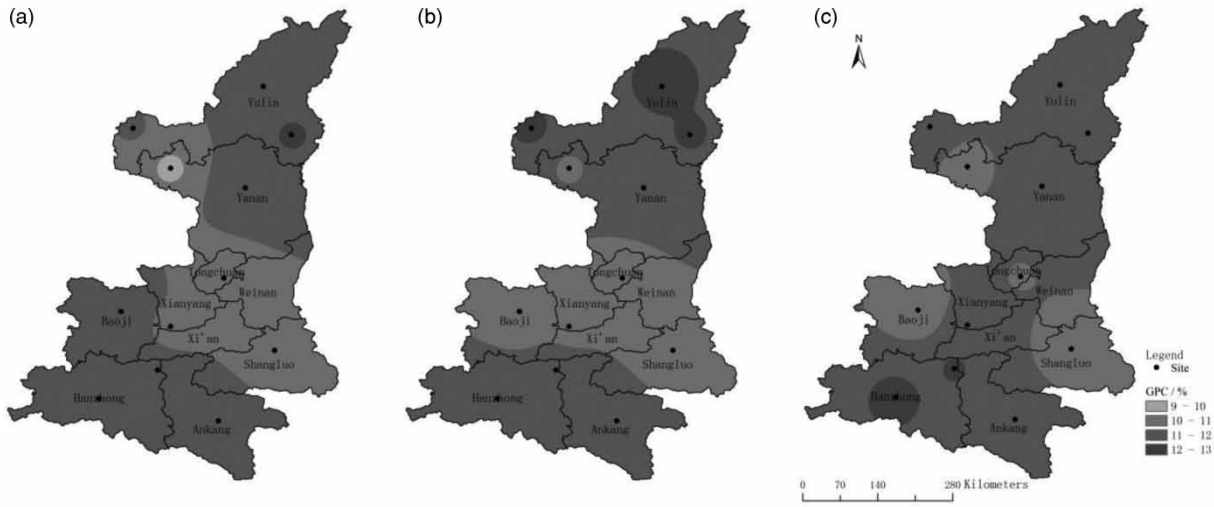

Figure 7 | GPC under rainfed conditions and historical climate data for 60 years (1957–2017) (a), radiative forcing at 4.5 Watts m^{-2} for 82 years (2018–2100) (b), and radiative forcing at 8.5 Watts m^{-2} for 82 years (2018–2100) (c).

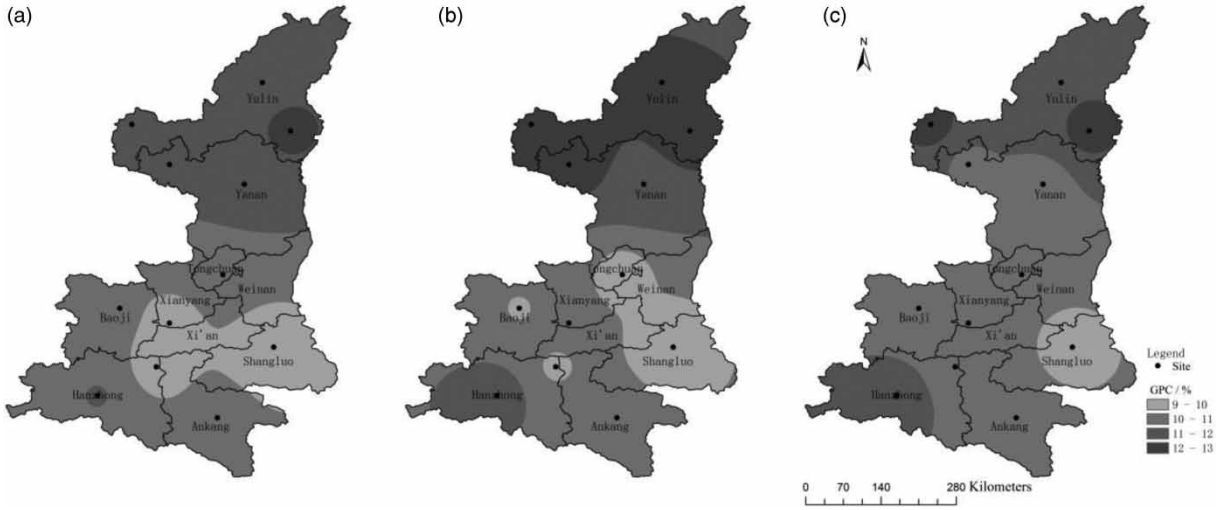

Figure 8 | GPC under irrigation conditions under the historical climate over 60 years (1957–2017) (a), radiative forcing at 4.5 Watts m^{-2} for 82 years (2018–2100) (b), and radiative forcing at 8.5 Watts m^{-2} for 82 years (2018–2100) (c).

decreased from 10.45 to 10.22%. The GPC of the semiarid region was much greater than that of the humid and subhumid regions. First, it increased from 11.76 to 12.41%, and it then decreased to 11.77%.

The risk to GPC in the humid region, subhumid region, and semiarid region decreased under SSP2-4.5 by 14.8, 9.9, and 23.8%, respectively (Figure 9(a)). The risk to GPC in the humid region, subhumid region, and semiarid region decreased under RCP by SSP5-8.5 27.2, 21.6 and 7.3%, respectively. The risk to GPC in the humid regions with irrigation increased greatly by 26.0% under the historical climate, 28.9% under SSP2-4.5 and 25.8% under SSP5-8.5 (Figure 9(b)). The risk to GPC in the subhumid areas with irrigation only increased 3.9% under the historical climate, 5.9% under SSP2-4.5 and 8.8% under SSP5-8.5. The risk to GPC in the semiarid regions with irrigation decreased by 24.25% under the historical climate, by 20.1% under SSP2-4.5 and by 9.9% under SSP5-8.5.

Downloaded from http://iwaponline.com/jwcc/article-pdf/12/6/2444/935000/jwc0122444.pdf
by guest

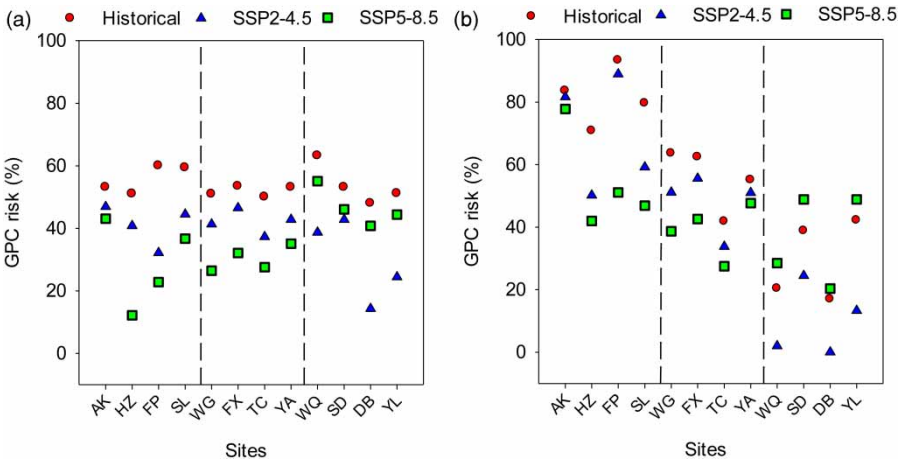

Figure 9 | Risk to GPC under rainfed conditions (a) and irrigation (b) under the historical climate over 60 years (1957–2017) (●), radiative forcing at 4.5 Watts m^{-2} for 82 years (2018–2100) (SSP2-4.5) (▲), and radiative forcing at 8.5 Watts m^{-2} for 82 years (2018–2100) (SSP5-8.5) (■).

DISCUSSION

Future wheat yield and quality in China will be threatened by climate change. A decline in GPC across fields from 1988 to 2012 has been attributed to climate change (Peltonen-Sainio *et al.* 2015). Rising temperatures that shortened the growing period were the main impact on wheat yields (Asseng *et al.* 2015). However, Asseng *et al.* (2019) also reported that GPC and yield increased in the warmer climates.

In this study, we first used modified CERES-Wheat to simulate GPC using the nitrogen-to-protein conversion factor. Then, CanESM5 was selected to simulate daily meteorological data, and SDSM was used to downscale the data. Modified CERES-Wheat was combined with the simulated meteorological data to simulate the future wheat yield and quality in Shaanxi. The temperature and precipitation increased under SSP2-4.5 and SSP5-8.5. It is generally acknowledged that a temperature increase is beneficial to GPC, whereas increases in precipitation and irrigation are beneficial to yield but harmful to GPC (Horstmann 2008). How yield and GPC change still needs further study. An irrigation scenario was also used as part of the strategy for responding to climate change. In the CERES-Wheat and other crop models, there was a correlation between photosynthetic intensity and CO_2 (Jones *et al.* 2003). Therefore, the yield was too high, and the GPC was too low, which differed from the actual situation. The mechanism by which crop growth responds to increases in CO_2 is uncertain (Asseng *et al.* 2019). Thus, increasing CO_2 was not considered as a factor in this study, which may make the results uncertain.

Evaluation of the simulation of GPC and yield

An accurate simulation of phenology ensured wheat-filling duration, which is the foundation of the accumulation of protein and dry matter, and the simulated yield was underestimated without nitrogen fertilization (N0). Yao *et al.* (2015) revealed that CERES-Wheat undervalues the capacity to resist stress.

The simulation of GPC was very good with severe water and nitrogen stress because GPC is the ratio of grain yield to grain nitrogen yield. The accumulation of nitrogen and dry matter during the grain-filling stage is more affected by temperature than by water and nitrogen stress (Ritchie & Otter 1985). However, the simulated results of the GPC with slight nitrogen stress (N1) were overestimated. Asseng *et al.* (2002) found that the accumulation rate of nitrogen was overestimated when the average temperature was less than 10 °C.

Effects of climate change and irrigation on yield and risk

Precipitation and temperature increased with climate change, but the yields of the different climatic regions

Downloaded from http://iwaponline.com/jwcc/article-pdf/12/6/2444/935000/jwc0122444.pdf
by guest

responded differently to climate change (Mubeen *et al.* 2019). Water supply had an extremely significant positive correlation with yield for all of the climatic regions. Water supply will play a dominant role in determining future winter wheat yield (Wang *et al.* 2011). The rising temperature could cause an increase in ET, and if the increase in precipitation is insufficient, then drought stress will be stronger (Panozzo *et al.* 2014).

In comparison to the other regions, the humid region had greater water and heat resources. Temperature and water were not the most important limiting factors for this region. The temperature and precipitation increased, but the yield only slightly decreased or increased. The reason may be that the yield in the humid region was at a relatively higher level and had largely reached the potential yield, and the excess precipitation decreased radiation. The study of Wang *et al.* (2012) showed similar results: reference crop evapotranspiration and crop-water requirements significantly decreased under climate change. Irrigation was still good for yield but only played a limited role. The temperature in the subhumid region increased and precipitation decreased under SSP2-4.5, while the winter wheat yields increased. Zhang & Yan (2003) recognized that although precipitation decreased, the appropriate increase in temperature promoted the growth of winter wheat. Radiation and temperature had higher suitability for yield in the subhumid region than in the other regions, and these factors increased under climate change (Jing & Fu-ning 2013). Decreasing precipitation became the main limiting factor for wheat yield, and water could not match the increasing temperature. Much radiation was wasted. Thus, the increasing yield was mainly due to irrigation.

The main limiting factors on yield in the semiarid region were low temperature and a shortage of water. Climate and cultivation conditions were not conducive to the growth of winter wheat. Climate change could compensate for these inadequacies. Winter wheat is suitable for high altitude and high latitude areas under the effects of climate change (Zheng *et al.* 2017). The influence of irrigation was greater than that of the other factors. The effects of climate change increased the yield only slightly, but irrigation exponentially increased the yield. Water was still the greatest limiting factor in terms of yield.

The decrease in precipitation in the humid regions was the main reason that the yield risk increased. The increasing temperature and precipitation remained stable, and the risk to yield in the other regions decreased. Furthermore, the changes in the frequency of extreme climatic events also increased yield risk (Semenov *et al.* 2007). Water was still the main limiting factor affecting yield risk (Moriondo *et al.* 2011), and of the agricultural measures to adapt crop growth to climate change, irrigation was the best option in all regions.

Effects of climate change and irrigation on GPC

Temperature and precipitation increased with increasing latitude, but the GPC decreased first and then increased. High temperatures can affect the formation of carbohydrates and proteins, influencing both the GPC and yield. The optimum temperature for grain dry matter accumulation is $20.7 \pm 1.4\,^{\circ}C$ during the grain-filling period (Porter & Gawith 1999), and the optimum temperature for grain nitrogen accumulation is $35\,^{\circ}C$ (Jones *et al.* 2003). At temperatures $>30\,^{\circ}C$, the rate of starch accumulation decreases, resulting in a higher GPC (Jenner 1994a). The humid region was relatively more suitable for the accumulation of protein, and the subhumid region was more suitable for the accumulation of dry matter. The semiarid region had temperature and precipitation that were lower than optimal, and elevated temperature and precipitation were beneficial to the accumulation of protein and dry matter in this region.

The GPC of the humid and semiarid regions increased slightly under SSP2-4.5 and SSP5-8.5, but the reasons for the increase were not the same. A relatively higher temperature in a humid region accelerates the rate of nitrogen accumulation in the grain and shortens the period of starch accumulation (Singh & Majumdar 2015). However, in a semiarid region, a relatively lower temperature and less precipitation limit the accumulation of nitrogen and dry matter. Climate change eases cold stress and drought stress and promotes both yield and GPC (Stone & Nicolas 1996; Wesley *et al.* 2001). In the subhumid region, the GPC decreased under SSP2-4.5 and SSP5-8.5. The increasing yield in the subhumid region was the greatest because of the suitable climate under SSP2-4.5 and SSP5-8.5. The

Downloaded from http://iwaponline.com/jwcc/article-pdf/12/6/2444/935000/jwc0122444.pdf
by guest

GPC was diluted by the excess dry matter in the grain (Li *et al.* 2011).

Irrigation further promoted yield, and GPC continuously decreased. The GPC of the subhumid region decreased slightly with climate change, and the GPC of the humid and subhumid regions declined markedly with irrigation. Thus, the commercial and economic aspects of the GPC were poor. Thus, it was recommended to reduce the amount of irrigation in the humid and subhumid regions. Adequate water could mitigate the effects of heat stress. Irrigation improved the rate of nitrogen uptake, but the GPC decreased with increasing yield (Zhang 2008). The accumulation of protein is independent of grain dry matter accumulation, but additional dry matter dilutes GPC (Groos *et al.* 2003). The GPC had a negative correlation with yield in the humid and subhumid regions, making it difficult to develop an effective management strategy to maximize profit. Irrigation was not suitable in the humid region. The contribution of irrigation to yield was limited, but the GPC decreased in the humid region. Irrigation was the primary reason for NO_3-N leaching (Min *et al.* 2000), and irrigation had a dilution effect on GPC (Yan *et al.* 2011).

Irrigation in the semiarid region promoted yield and GPC. Xu and Yu recognized that severe water stress decreases the photosynthetic rate and nitrogen concentration and that irrigation plays an important role in the improvement of grain quality and yield in semiarid regions (Xu & Yu 2006).

The risk to GPC in all the regions decreased with climate change. The accumulation of grain protein and starch during the grain-filling period was two independent processes (Vos 1981). The starch accumulation rate decreased when the temperature was above 30 °C, while the grain protein accumulation rate was largely unaffected (Jenner 1994b; Altenbach *et al.* 2003). The grain protein accumulation was determined by temperature (Jones *et al.* 2003), so the GPC risk under SSP5-8.5 was less than that under SSP2-4.5. Irrigation increased grain starch, and increasing temperature increased grain protein. The comprehensive effects of irrigation and increasing temperature caused different results in the three climatic regions. Of the factors, irrigation had the greatest effect on the yield of the humid region, and irrigation and increasing temperature had the same effect on the yield of the semi-humid region. Low temperature was the main limiting factor for the semiarid region.

CONCLUSIONS

This study simulated and evaluated the risk of climate change and irrigation to yield and quality using a crop model and representative concentration pathways. The GPC and yield risks had different responses to climate change and irrigation, and irrigation should be discreetly applied for different climatic regions to combat climate change. The methodology allowed us to assess the risk to wheat yield and quality shortfalls from climate change and irrigation by assigning probability estimates as opposed to providing only uncertainty ranges.

1. Temperature and precipitation increased. Elevated temperature and precipitation had positive effects on yield in all regions. The risk to yield in most regions with climate change decreased by 3.8–25.1%.
2. In the humid and semiarid regions, GPC increased under SSP2-4.5 and SSP5-8.5. However, in the subhumid region, it decreased. The risk to GPC in all regions under SSP2-4.5 and SSP5-8.5 decreased 7.3–27.2%.
3. Irrigation decreased the risk to yield greatly in all regions but had totally different effects in the three climatic regions. The risk to yield with irrigation decreased 37.7–52.1% in different climates. The risk to GPC with irrigation increased greatly by 25.8–28.9% in the humid region and by 3.9–8.8% in the subhumid region and decreased by 37.7–52.1% in the semiarid region.

DATA AVAILABILITY STATEMENT

All relevant data are included in the paper or its Supplementary Information.

REFERENCES

Addo, K., Pomeranz, Y., Huang, M. L., Rubenthaler, G. L. & Jeffers, H. C. 1991 Steamed bread. II. Role of protein content and strength. *Cereal Chemistry* **68**, 39–42.

Downloaded from http://iwaponline.com/jwcc/article-pdf/12/6/2444/935000/jwc0122444.pdf
by guest

Ahmad, M. J., Cho, G. H., Kim, S. H., Lee, S. & Choi, K. S. 2020 Influence mechanism of climate change over crop growth and water demands for wheat-rice system of Punjab, Pakistan. *Journal of Water and Climate Change* **6**, 1–18.

Albert, W., Cynthia, J. H. & Jaepil, W. 2003 Assessing winter wheat responses to climate change scenarios: a simulation study in the U.S. Great Plains. *Climatic Change* **58** (1–2), 119–147.

Allen, L. H., Kimball, B. A., Bunce, J. A., Yoshimoto, M. & White, J. W. 2020 Fluctuations of CO_2 in free-air CO_2 enrichment (FACE) depress plant photosynthesis, growth, and yield. *Agricultural and Forest Meteorology* **284**, 107899.

Altenbach, S. B., Dupont, F. M., Kothari, K. M., Chan, R., Johnson, E. L. & Lieu, D. 2003 Temperature, water and fertilizer influence the timing of key events during grain development in a US spring wheat. *Journal of Cereal Science* **37** (1), 9–20.

Asseng, S., Bartal, A., Bowden, J. W., Ba, V. H. A., Palta, J. A., Huth, N. I. & Probert, M. E. 2002 Simulation of grain protein content with APSIM-Nwheat. *European Journal of Agronomy* **16** (1), 25–42.

Asseng, S., Ewert, F., Rosenzweig, C., Jones, J. W., Hatfield, J. L., Ruane, A. C., Boote, K. J., Thorburn, P. J., Rötter, R. P. & Cammarano, D. 2013 Uncertainty in simulating wheat yields under climate change. *Nature Climate Change* **3** (9), 827–832.

Asseng, S., Ewert, F., Martre, P., Rötter, R. P., Lobell, D. B., Cammarano, D., Kimball, B. A., Ottman, M. J., Wall, G. W. & White, J. W. 2015 Rising temperatures reduce global wheat production. *Nature Climate Change* **5** (2), 143.

Asseng, S., Martre, P., Maiorano, A., Rötter, R. P., O Leary, G. J., Fitzgerald, G. J., Girousse, C., Motzo, R., Giunta, F. & Babar, M. A. 2019 Climate change impact and adaptation for wheat protein. *Global Change Biology* **25** (1), 155–173.

Bai, H., Xiao, D., Wang, B., Liu, D., Feng, P. & Tang, J. 2021 Multimodel ensemble of CMIP6 projections for future extreme climate stress on wheat in the North China plain. *International Journal of Climatology* **41** (Suppl. 1), 171–186.

Dubey, M., Mishra, A. & Singh, R. 2020 Climate change impact analysis using bias-corrected multiple global climate models on rice and wheat yield. *Journal of Water and Climate Change* **2**, 1–14.

Eyring, V., Bony, S., Meehl, G., Senior, A. & Catherine and, A. 2016 *Overview of the Coupled Model Intercomparison Project Phase 6 (CMIP6) Experimental Design and Organization*. Geoscientific Model Development.

Gaffin, S. R., Rosenzweig, C., Xing, X. & Yetman, G. 2004 Downscaling and geo-spatial gridding of socio-economic projections from the IPCC special report on emissions scenarios (SRES). *Global Environmental Change* **14** (2), 105–123.

Garofalo, P., Ventrella, D., Kersebaum, K. C., Gobin, A., Trnka, M., Giglio, L., Dubrovský, M. & Castellini, M. 2019 Water footprint of winter wheat under climate change: trends and uncertainties associated to the ensemble of crop models. *Science of the Total Environment* **658**, 1186–1208.

Gilardelli, C., Confalonieri, R., Cappelli, G. A. & Bellocchi, G. 2018 Sensitivity of WOFOST-based modelling solutions to crop parameters under climate change. *Ecological Modelling* **368**, 1–14.

Groos, C., Robert, N., Bervas, E. & Charmet, G. 2003 Genetic analysis of grain protein-content, grain yield and thousand-kernel weight in bread wheat. *Theoretical & Applied Genetics* **106** (6), 1032–1040.

He, J., Dukes, M. D., Jones, J. W., Graham, W. D. & Judge, J. 2009 Applying GLUE for estimating CERES-MAIZE genetic and soil parameters for sweet corn production. *Transactions of the ASABE* **52** (6), 1907–1921.

Horstmann, B. 2008 *Framing Adaptation to Climate Change – A Challenge for Building Institutions*. Deutsches Institut für Entwicklungspolitik gGmbH, Bonn.

IPCC 2013 Climate change 2013: the physical science basis. *Contribution of Working* **43** (22), 866–871.

Jabeen, M., Gabriel, H. F., Ahmed, M., Mahboob, M. A. & Iqbal, J. 2017 Studying impact of climate change on wheat yield by using DSSAT and GIS: a case study of Pothwar region. In: *Quantification of Climate Variability, Adaptation* (M. Ahmed & C. O. Stockle, eds.). Springer, Cham, pp. 387–411.

Jenner, C. F. 1994a Starch synthesis in the kernel of wheat under high temperature conditions. *Functional Plant Biology* **21** (6), 791–806.

Jenner, C. F. 1994b Starch synthesis in the kernel of wheat under high temperature conditions. *Functional Plant Biology* **21** (6), 791–806.

Jing, X. & Fu-Ning, Z. 2013 Impact of demographic transition on food demand in china: 2010–2050. *China Population, Resources and Environment* **23** (6), 117–121.

Jones, J. W., Hoogenboom, G., Porter, C. H., Boote, K. J., Batchelor, W. D., Hunt, L. A., Wilkens, P. W., Singh, U., Gijsman, A. J. & Ritchie, J. T. 2003 The DSSAT cropping system model. *European Journal of Agronomy* **18** (3–4), 235–265.

Li, Y., Yin, Y., Zhao, Q. & Wang, Z. 2011 Changes of glutenin subunits due to water–nitrogen interaction influence size and distribution of glutenin macropolymer particles and flour quality. *Crop Science* **51** (6), 2809.

Liu, J., Feng, H., He, J., Chen, H. & Ding, D. 2018 The effects of nitrogen and water stresses on the nitrogen-to-protein conversion factor of winter wheat. *Agricultural Water Management* **210**, 217–223.

Mckenzie, R. H., Bremer, E., Grant, C. A., Johnston, A. M., Demulder, J. & Middleton, A. B. 2006 In-crop application effect of nitrogen fertilizer on grain protein concentration of spring wheat in the Canadian Prairies. *Canadian Journal of Soil Science* **86** (86), 565–572.

Meenu, R., Rehana, S. & Mujumdar, P. P. 2013 Assessment of hydrologic impacts of climate change in Tunga-Bhadra basin, India with HEC-HMS and SDSM. *Hydrobiological Processes* **27** (11), 1572–1589.

Meng, Z. J., Duan, A. W., Dassanayake, K. B., Chen, D. L., Gao, Y., Wang, X. S. & Shen, X. J. 2016 Effects of regulated deficit irrigation on grain yield and quality traits in winter wheat. *Transactions of the ASABE* **59** (3), 897–907.

Downloaded from http://iwaponline.com/jwcc/article-pdf/12/6/2444/935000/jwc0122444.pdf
by guest

Min, Y. X., An, T. Y., Yun, Y. X., Lin, L. X. & Suo, Z. F. 2000 Effect of irrigation and precipitation on soil nitrate nitrogen accumulation. *Journal of Soil Water* **14** (3), 71–73.

Moriondo, M., Giannakopoulos, C. & Bindi, M. 2011 Climate change impact assessment: the role of climate extremes in crop yield simulation. *Climatic Change* **104** (3–4), 679–701.

Mubeen, M., Ahmad, A., Hammad, H. M., Awais, M. & Nasim, W. 2019 Evaluating the climate change impact on water use efficiency of cotton-wheat in semi-arid conditions using DSSAT model. *Journal of Water and Climate Change* **11** (4), 1661–1675.

Nuttall, J. G., O'Leary, G. J., Panozzo, J. F., Walker, C. K., Barlow, K. M. & Fitzgerald, G. J. 2017 Models of grain quality in wheat – a review. *Field Crops Research* **202**, 136–145.

Omenn, G. 1997 Framework for environmental health risk management: final report. In: *Presidential/Congressional Commission on Risk Assessment and Risk Management*.

O'Neill, B. C., Kriegler, E., Riahi, K., Ebi, K. L., Hallegatte, S., Carter, T. R., Mathur, R. & Vuuren, D. P. 2014 A new scenario framework for climate change research: the concept of shared socioeconomic pathways. *Climatic Change* **122** (3), 387–400.

Panozzo, J., Cassandra, K. W., Partington, D. L., Neumann, N. C., Tausz, M. & Seneweera, S. 2014 Elevated carbon dioxide changes grain protein concentration and composition and compromises baking quality. A FACE study. *Journal of Cereal Science* **60** (3), 461–470.

Peltonen-Sainio, P., Salo, T., Jauhiainen, L., Lehtonen, H. & Sieviläinen, E. 2015 Static yields and quality issues: is the agri-environment program the primary driver? *Ambio* **44** (6), 544–556.

Pleijel, H., Broberg, M. C., Uddling, J. & Mills, G. 2018 Current surface ozone concentrations significantly decrease wheat growth, yield and quality. *Science of the Total Environment* **613–614**, 687–692.

Porter, J. R. & Gawith, M. 1999 Temperatures and the growth and development of wheat: a review. *European Journal of Agronomy* **10** (1), 23–36.

Priestley, C. H. B. & Taylor, R. J. 1972 On the assessment of surface heat flux and evaporation using large scale parameters. *Monthly Weather Review* **100** (2), 81–92.

Qing, W. U., Jiang, X. & Xie, J. 2017 Evaluation of surface air temperature in southwestern China simulated by the CMIP5 models. *Plateau Meteorology* **36** (2), 358–370.

Rajabi, A. & Shabanlou, S. 2015 The analysis of climate change uncertainty by means of SDSM model (case study: Kermanshah province, Iran). *Agricultural Communications* **3** (3), 33–40.

Ritchie, J. R. & Otter, S. 1985 Description and performance of CERES-Wheat: a user-oriented wheat yield model. *ARS Wheat Yield Project* **38**, 158–175.

Rodríguez-Félix, F., Ramirez-Wong, B., Torres-Chávez, P. I., álvarez-Avilés, A. & Sergio-Moreno-Salazar, S. 2014 Yellow berry, protein and agronomic characteristics in bread wheat under different conditions of nitrogen and irrigation in northwest Mexico. *Pakistan Journal of Botany* **46** (1), 221–226.

Schmidli, J., Frei, C. & Vidale, P. L. 2006 Downscaling from GCM precipitation: a benchmark for dynamical and statistical downscaling methods. *International Journal of Climatology* **26** (5), 679–689.

Semenov, S., Patwardhan, A., Burton, I., Oppenheimer, M., Pittock, A. B., Rahman, A., Smith, J. B., Yamin, F., Parry, M. L. & Canziani, O. F. 2007 Assessing key vulnerabilities and the risk from climate change. In: *Chapter 19 in the Intergovernmental Panel on Climate Change Fourth Assessment Report, Working Group II: Impacts, Adaptation and Vulnerability*, pp. 779–810.

Singh, I. R. & Majumdar, S. P. 2015 Effects of nutrients and compaction levels on amino acids and protein content in wheat (*Triticum aestivum* L.) grain. *International Journal of Agricultural Sciences* **11** (1), 1–6.

Song, Y., Qiao, F., Song, Z. & Jiang, C. 2013 Water vapor transport and cross-equatorial flow over the Asian-Australia monsoon region simulated by CMIP5 climate models. *Advances in Atmospheric Sciences* **30** (3), 726–738.

Stone, P. J. & Nicolas, M. E. 1996 Varietal differences in mature protein composition of wheat resulted from different rates of polymer accumulation during grain filling. *Functional Plant Biology* **23** (6), 727–737.

Swart, N. C., Cole, J. N. S., Kharin, V. V., Lazare, M. & Winter, B. 2019 The Canadian Earth System Model version 5 (CanESM5). *Geoscientific Model Development* **12** (11), 4823–4873.

Timbal, B., Dufour, A. & Mcavaney, B. 2003 An estimate of future climate change for western France using a statistical downscaling technique. *Climate Dynamics* **20** (7–8), 807–823.

Vos, J. 1981 *Effects of Temperature and Nitrogen Supply on Post-Floral Growth of Wheat; Measurements and Simulations*. Landbouwhogeschool.

Wang, J., Li, W. E. & Liu, D. L. 2011 Modelling the impacts of climate change on wheat yield and field water balance over the Murray–Darling Basin in Australia. *Theoretical and Applied Climatology* **104** (3–4), 285–300.

Wang, W. G., Peng, S. Z., Sun, F. C., Xing, W. Q. & Xu, J. Z. 2012 Spatiotemporal variations of rice irrigation water requirements in the mid-lower reaches of Yangtze river under changing climate. *Advances in Water Science* **23** (5), 656–664.

Wesley, A. S., Lukow, O. M., Rih, M. K., Ames, N. & Brown, D. 2001 Effect of multiple substitutions of glutenin and gliadin proteins on flour quality of Canada Prairie Spring. *Cereal Chemistry* **78** (1), 69–73.

Wong, L. T. & Chow, W. K. 2001 Solar radiation model. *Applied Energy* **69** (3), 191–224.

Worku, T., Khare, D. & Tripathi, S. K. 2018 Spatiotemporal trend analysis of rainfall and temperature, and its implication on crop production. *Journal of Water & Climate Change* **10** (4), 799–817.

Downloaded from http://iwaponline.com/jwcc/article-pdf/12/6/2444/935000/jwc0122444.pdf
by guest

Xin, C. H. 2017 *Effects of Different Mulching Applications on Greenhouse Gas Emissions and Their Responds on Future Climate Change Scenrios*. Northwest A&F University.

Xu, Z. & Liu, Z. 2014 *Climate Change Scenarios and the Impact on Runoff*. Springer Netherlands, New York.

Xu, Z. Z. & Yu, Z. W. 2006 Nitrogen metabolism in flag leaf and grain of wheat in response to irrigation regimes. *Journal of Plant Nutrition and Soil Science* **169** (1), 118–126.

Yan, J. D., Wen, Y. Z. & Zhu, X. Z. 2011 Effects of irrigation amount and nitrogen fertilization rate on wheat yield and soil nitrate content. *Chinese Journal of Applied Ecology* **22** (2), 364–368.

Yao, N., Zhou, Y., Song, L., Liu, J., Li, Y., Wu, S., Feng, H. & He, J. 2015 Parameter estimation and verification of DSSAT-CERES-Wheat model for simulation of growth and development of winter wheat under water stresses at different growth stages. *Transactions of the Chinese Society of Agricultura* **31** (12), 138–150.

Zhai, W., Pengjun, L. I., Lin, K. & Zhang, F. 2016 The prediction of climatic change and runoff response in the Dongjiang Basin based on SDSM-SWAT model. *Pearl River* **37** (4), 1–6.

Zhang, Y. L. 2008 Effects of irrigation amount on the nitrogen uptake, distribution, use, grain yield and quality in wheat. *Acta Agronomica Sinica* **34** (5), 870–878.

Zhang, J. X. & Yan, J. P. 2003 Evaluation model of wheat yield in regional response to climate change. *Journal of Arid Land Resources and Environment* **17** (1), 85–90.

Zhang, Q., Qi, D., Dong, X., Li, X., Cheng, L., Liu, H., Chen, S., Rajora, O. P., Li, X. & Liu, G. 2020 Amino acid composition, protein content and accurate nitrogen-to-protein conversion factor for sheepgrass (*Leymus chinensis*). *Botany* **98** (3), 137–146.

Zheng, L. F., Shang, Y. F., Li, X. J., Feng, H. & Wei, Y. S. 2017 Structural equation model for analyzing relationship between yield and agronomic traits in winter wheat. *Acta Agronomica Sinica* **43** (9), 1395–1400.

First received 18 August 2020; accepted in revised form 8 March 2021. Available online 23 March 2021

Downloaded from http://iwaponline.com/jwcc/article-pdf/12/6/2444/935000/jwc0122444.pdf
by guest